Structural Eng./Earthquake Eng., JSCE, Vol. 19, No. 1, 11s—20s, 2002 January
(J. Struct. Mech. Earthquake Eng., JSCE, No. 696/ I —58)

INELASTIC SEISMIC RESPONSE OF BRIDGE PILES: EFFECTS OF SUPERSTRUCTURE PROPERTIES AND SOIL LAYERING

Jorge SHIMABUKU[1] and Hirokazu TAKEMIYA[2]

[1]Member of JSCE, Ph.D., Foreign Researcher , Dept. of Env. and Civil Eng., Okayama University
(Tsushima Naka 3-1-1, Okayama-shi, Okayama-ken, 700-8530, Japan)
[2]Member of JSCE, Dr. Eng., Professor, Dept. of Env. and Civil Eng., Okayama University
(Tsushima Naka 3-1-1, Okayama-shi, Okayama-ken, 700-8530, Japan)

This paper has dealt with the nonlinear behavior of pile-supported bridge during earthquake motions. The formulation takes the FEM-BEM technique; the FEM for the near structure zone while the BEM for the far field zone. The analyses addressed to the parameter studies of component influence on the behavior of the total superstructure-pile-soil system for the total rational design practice. The results are interpreted with regards to: (1) inelastic behavior of superstructure or/and substructure; (2) different superstructure properties and vertical excitation conditions; and (3) soil layering effect on pile response with emphasis on kinematic and inertial interactions.

Key Words : *soil-pile interaction, nonlinear behavior, layered soil, vertical excitation, inertial and kinematic interaction, maximum displacement profile, internal forces in piles profile*

1. INTRODUCTION

Structures sited on soft soils are founded by deep foundations. Pile foundations are widely used in order to transfer superstructural weight to the sound bearing bottom layer at depth. In addition to this, the pile design is demanded of the lateral resistance against earthquake loading, as have been evidenced in the highway bridges in recent strong earthquakes. Because of the difficulties for identifying damage degrees of piles and for repairing them after such events, the general design philosophy is to ensure that piles response should remain in the elastic range to voiding damages. However, from field investigation it was found hard for piles to be escaped in the Hyogoken Nanbu Earthquake from the inelastic behavior. One worst case reported was the piles failure due to the coupled shear and bending action, wheras the superstructure remained intact[1),2)].

A general design feature of highway bridges at soft sites is a top-heavy structure supported by the piles. The action of the axial force in piles leads the modifications of their degrading flexural characteristic. Although numerous works have been reported on the dynamic superstructure-pile-soil interaction (SPSI), the detailed studies on the behavior of the piles under the varying axial loads are still needed.

Investigations of the inelastic interaction of one comprising element with another element are the main objective of this paper. Especially, the nonlinear pile behavior in stratified soil profile[3)-6)] is dealt. The following specific issues are targeted herein: (1) characteristics of structural response due to inelastic behavior of superstructure (pier) or/and substructure (pile foundation); (2) variation of structural behavior due to different superstructure properties and for vertical excitation in addition to the horizontal input; and (3) effects of soil layering on pile response with the emphasis on kinematic and inertial interactions. The findings based on the parameter studies may potentially contribute to the more sound and economical design practice of highway bridges.

2. METHODOLOGY

Dynamics of soil-structure interaction are considered by using a two-dimensional (2-D) nonlinear model based on the time domain FEM-BEM (Finite Element Method and Boundary Element Method) hybrid technique[7)]. The FE region

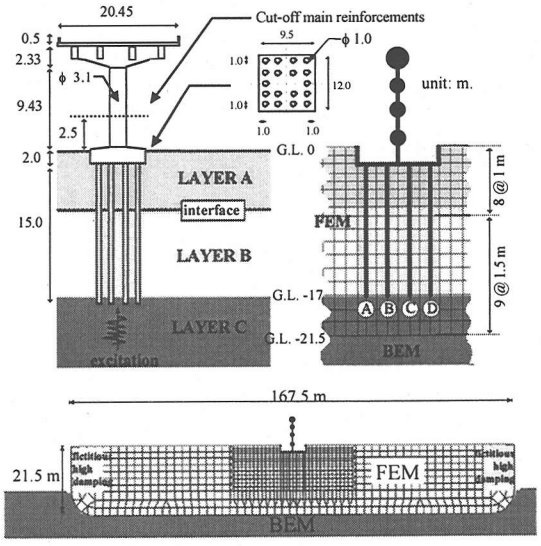

Fig.1 Typical bridge of the Japanese Highway network and its model of analysis.

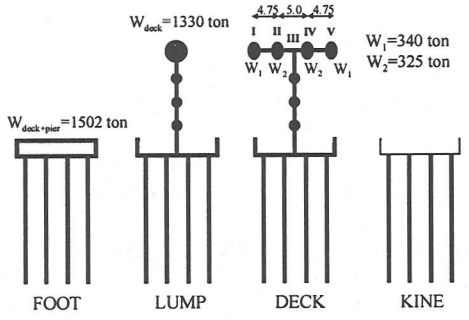

Fig.2 Modeling for parametrical study.

Table 1 Studied profiles.

	Case / Layer	Soil-11	Soil-21	Soil-12	Soil-22	Soil-12-s	Soil-21-s	Soil-12-d
Shear velocity V_s (m/s)	A	100	200	100	200	100	200	100
	B		100	200		200	100	200
Density ρ (t/m^3)	A	1.5	1.6	1.5	1.6	1.5	1.6	1.5
	B		1.5	1.6		1.6	1.5	1.6
Poisson's ratio ν	A	0.45	0.37	0.45	0.37	0.45	0.37	0.45
	B		0.45	0.37		0.37	0.45	0.37
Distance from pile top to interface (m)		---	5	5	---	2	2	9

is assumed as a non-homogeneous nonlinear zone while the BE region is taken as a linearly elastic zone. Therefore, the deeper stiff soil is included in the BE zone. The pier and piles are discretized by the conventional beam elements. The neighboring soil is represented by the FE and the vertical side boundary is located at far distance from the zone of interest. Moreover, fictitious high damping coefficients are imposed to the FE soil edge elements in order to let them absorb the outgoing waves.

The soil nonlinear behavior is characterized by the Mohr stress circle criterion and the hyperbolic model originally proposed by Hardin and Drnevich[8], which was refined by Takemiya *et al.*[9] to be more suitable for a computational simulation in 2-D problems for irregular seismic motions. The equation of motion of the total system is solved step-by-step by the Newmark method by taking care of the nonlinearity by the iterative Newton-Raphson procedure.

The inelastic behavior of RC beam elements are represented by the one component model proposed by Giberson[10] but including both sway and rotational motion at both ends of each element as formulated by Takemiya and Shimabuku.[11] The RC hysteresis model is treated by the Q-hyst model[12], which was modified to take into account of the relationship between bending moment and axial force.[13] The axial load is counted for in evaluating the yield bending moment at each computational step from the bending moment-axial force interaction diagram. These are implemented into the previous computer code for the soil nonlinear behavior[7].

3. MODELS FOR ANALYSIS

The structure analyzed in this paper is a typical bridge of Highway viaducts in Japan. **Fig.1** shows an illustration for it and the model for analysis. The rows of piles are grouped as A, B, C and D for reference. The length of pile elements is taken identical with the size of soil elements. The bottom BEM boundary is set at G.L. –21.5 m and the vertical side boundaries are located at 83.75 m from the center of footing. In order to meet with the plane strain assumption for the soil FEM model a compatible beam with this assumption should be considered by taking a properly chosen distance in the third direction[14]. The width of 24 m (twice of the footing width) is adopted in this direction herein.

For the convenience of parametrical analyses, four structural models are chosen as given in the illustration in **Fig.2**. The "FOOT" model includes the deck and pier masses in the footing FE solid elements. The "LUMP" model lumps the deck mass at the pier top by one node only for sway motion so that the deck moment of inertia is excluded. The "DECK" model incorporates deck mass as placed at the original position. Both "LUMP" and "DECK" models represent the footing by the equivalent beams. Finally, the "KINE" model considers a massless superstructure, only to evaluate the

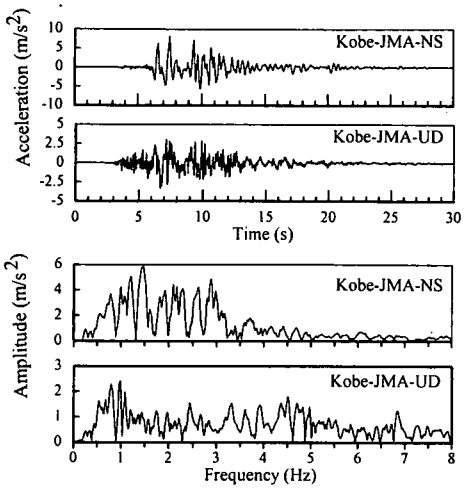

Fig.3 Kobe-JMA acceleration.

Table 2 Analyses for LUMP model.

Notation	Column (pier) type	Pile type	Soil type	Soil profile
LUMP-LC-LP	linear	linear	nonlinear	Soil-12
LUMP-LC-NP	linear	nonlinear		
LUMP-NC-LP	nonlinear	linear		
LUMP-NC-NP	nonlinear	nonlinear		

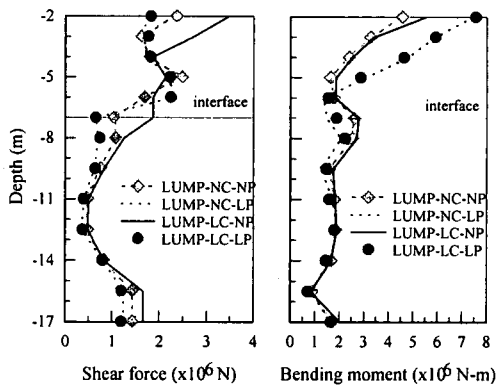

Fig. 4 Maximum internal forces for the LUMP model.

Table 3 Maximum responses at pier for LUMP model.

Internal forces	LUMP -LC-LP	LUMP -LC-NP	LUMP -NC-LP	LUMP -NC-NP
Bending moment at pier bottom (x10⁶ N-m)	180	165	102	104
Shear force at pier bottom (x10⁶ N)	16.3	15.1	28.3	25.6

kinematic response along the footing boundary with the surrounding soil. In the "KINE" model, the yield bending moment is calculated from the bending moment-axial force interaction diagram in view of the static axial load.

The geological site condition in **Fig.1** makes a stack of soil layers, which are denoted as LAYER A and B underlain by much stiffer soil LAYER C. LAYER C has the same properties with those of the extending linear half-space (BE); the shear velocity (Vs) of 600 m/s, the mass density (ρ) of 1.80 t/m^3 and the Poisson's ratio (ν) of 1/3 for all studied cases. The properties of the considered soil profiles (LAYER A and B) are given in **Table 1**. The identifier numbers in the profiles correspond to the LAYER A and LAYER B, respectively in the order. The number "1" refers to the layer of Vs=100 m/s and the number "2" to the layer of Vs=200 m/s. The letter "s" means that the interface of layers is located near the surface (G.L. -4 m) and the letter "d" indicates that the interface is placed at the depth (G.L. -11 m).

The system is excited by seismic motions observed at the Japan Meteorology Agency in Kobe during the1995 Hyogo-ken Nanbu Earthquake. **Fig.3** shows these measured accelerograms and their Fourier spectral densities. The acceleration record is transformed into the displacement record for the input motion.

4. EFFECTS OF PIER AND/OR PILE INELASTIC BEHAVIOR

The interrelation between superstructure and pile foundation is analyzed throughout the 4 cases listed in **Table 2** for different assumptions of behavior. Here, the linear behavior means that all the comprising elements remain always in the elastic range.

Fig. 4 shows the maximum shear forces and bending moments along the length of piles. The values of these figures are chosen from the maximum responses of all piles. When piles have linear properties, the differences between LUMP-NC-LP and LUMP-LC-LP responses are very small. This means that piles elastic responses are practically indifferent to type of behavior (elastic or inelastic) of the pier. However, when piles have nonlinear behavior, the effect of pier behavior is clearly noted especially close to the pile top. If a comparison is made between LUMP-LC-NP and LUMP-NC-NP, it is noted that the nonlinear behavior of pier leads to the smaller pile top forces, as caused by the hysteretic energy dissipation at the pier body that results in the reduction of the superstructure acceleration and consequently the inertial interaction effect. Since the maximum shear force value at pile top of the LUMP-LC-NP case is larger than the maximum shear capacity calculated from the "Seismic Design Specifications of Highway Bridges"[15], the shear failure can be important in addition to the bending type failure. At the pier bottom, the effects of the type of pile behavior (linear or nonlinear) are not clearly

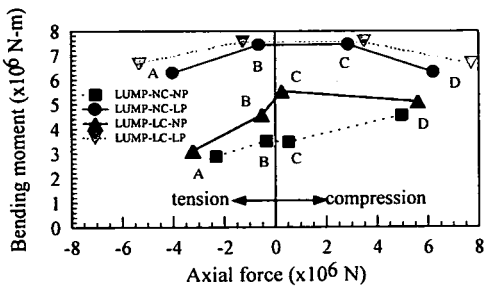

Fig. 5 Bending moment-axial force relationship at pile top when the respective pile attains the maximum bending moment.

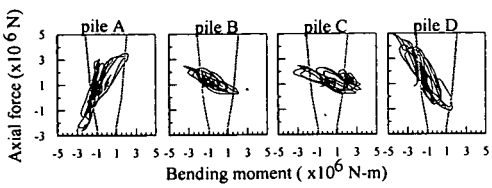

Fig. 6 Bending moment-axial force relationship at pile top for LUMP-NC-NP.

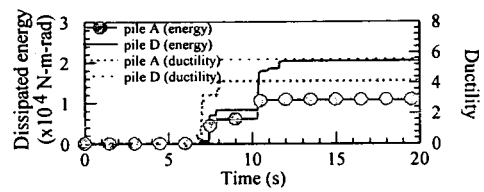

Fig. 7 Dissipated energy and ductility for LUMP-NC-NP.

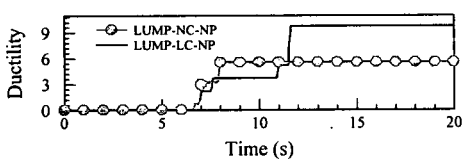

Fig. 8 Ductility at pile top with maximum bending moment.

Table 4 Cases for different superstructure characteristics.

CASE	Model	Pier height (m)	Input
F	FOOT	---	Kobe JMA-NS
L-6	LUMP	6	
L-9		9	
L-12		12	
L-15		15	
L-12-V		12	Kobe JMA-NS + JMA-UD
D-12	DECK	12	Kobe JMA-NS
D-12 (e=+1.5)			
D-12 (e=-1.5)			
D-12-V			Kobe JMA-NS + JMA-UD
D-12-V (e=-1.5)			

noticeable from **Table 3**.

Fig. 5 shows the bending moment-axial force relationship at the pile top when the respective pile attains the maximum bending moment. It is clear that the response has a symmetric shape when the pile is linear. In this case, very similar responses are obtained for the internal piles B and C and for the external piles A and D. In **Fig. 6**, the relationship between the axial force and bending moment is investigated in the time history. Here, the gray lines indicate the yield state. The pile A experiences the maximum tension force (negative value) and the pile D has the maximum compression force (positive value).

In addition to the peak response values, the rotational ductility is checked to evaluate the degrees of structural damage associated with the inelastic behavior. The rotational ductility is defined by the ratio of maximum rotation divided by the yield rotation for each component. **Fig.7** shows the dissipated energy and the ductility at the pile top for the LUMP-NC-NP case. The dissipated energy is summed up from of area inside of individual hysteresis loops. It is noted that the pile in maximum compression (pile D) has larger values than the pile in maximum tension force (pile A). Therefore, the possible failure of pile is due to the relation between compression force and bending moment rather than tension force and bending moment. **Fig. 8** shows the ductility at the pile top of LUMP-NC-NP and LUMP-LC-NP for piles of the maximum bending moment. The linear pier case (LUMP-LC-NP) attains the larger values than the nonlinear pier case (LUMP-NC-NP). Other interesting observation is that a sudden big increase (jump) for LUMP-LC-NP occurs between 10.9 s and 11.6 s, which include the time when the maximum bending moment at the pier bottom occurs at 11.23 s.

The response characteristic of the total system proved to be that the type of the pier behavior is strong effect in the pile response, but the reverse effect is small. However, it has to be taken care that other imposed ground motions might induce different responses to lead to different conclusions.

5. EFFECTS OF SUPERSTRUCTURE CHARACTERISTICS

Table 4 lists the studied cases to investigate the influence on the response of the deck rotational inertia, the deck eccentricity, the pier flexibility and the vertical excitation component. In these cases, the letter "V" indicates that the cases excited by the vertical input motion in addition to the horizontal. The letter "e" means that DECK model has a geometrical eccentricity in either direction. For all cases, the piles are embedded in the soil of profile Soil-12 (see **Table 1**). The effect of rocking due to the presence of superstructure is studied by comparing the F, L-12 and D-12 cases. The effect of vertical excitation is investigated by the L-12-V and

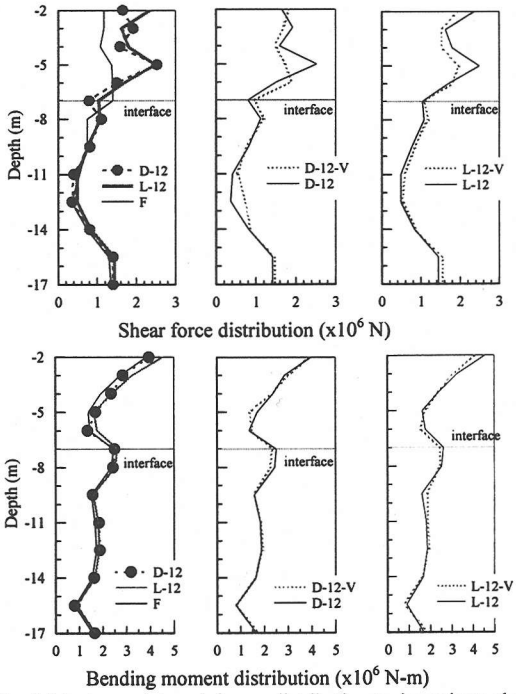

Fig. 9 Maximum internal forces distribution to investigate the deck rotational inertia and vertical excitation effects.

D-12-V cases. The deck eccentricity is considered in the D-12 (e=+1.5), D-12 (e=-1.5) and D-12-V (e=-1.5) cases. Different structural flexibilities are considered by giving different yield coefficients, defined as a horizontal yield load divided by the weight of superstructure. This yield coefficient is varied from 0.37 to 0.94 in the height of pier of the L-6, L-9, L-12 and L-15 cases.

(1) Deck rotational inertia and vertical excitation

The shear force and bending moment profiles along the length of pile are depicted in **Fig. 9**. The L-12 and D-12 cases attain the larger forces than the case F. While the case F has the maximum shear forces spread out between G.L. –5 m and G.L. –7 m, the D-12 and L-12 cases indicate a concentration around G.L. –5 m. The above observations are caused by the fact that the L-12 and D-12 cases take into account the overturning moment from the superstructure, which is not considered for the case F. Moreover, the shear force at the pile top of the L-12 case is larger than the D-12. This difference can be attributed to the fact that the footing horizontal displacement of the L-12 is larger than that of the D-12. The second mode of vibration of L-12 corresponds to the footing sway motion while the second mode of vibration of the D-12 to the deck rotation. Moreover, the double curvature of the pier of the D-12 leads a possible

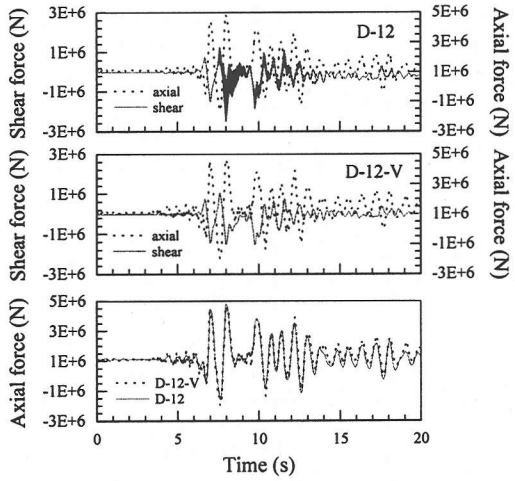

Fig. 10 Shear and axial force time histories of pile D at G.L. –5 m

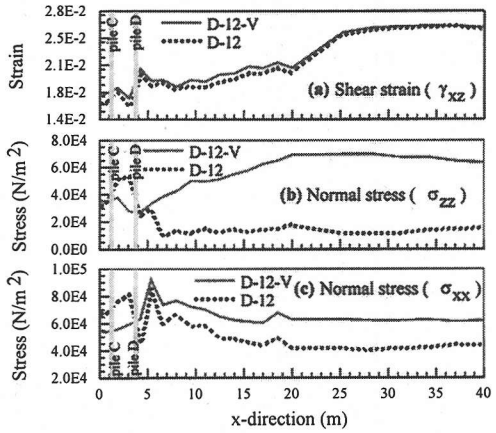

Fig. 11 Maximum responses in surrounding soil due to vertical excitation effect at G.L. –5 m.

inelastic behavior both at the top and bottom of pier. On the other hand, if shear force distribution of the L-12-V and D-12-V cases are compared with those of the L-12 and D-12 cases, a reduction is observed in the former cases at G.L. –5 m.

In order to investigate this reason, the shear and axial force time histories at the depth of 5 m are shown in **Fig. 10**. In this figure and the following, the positive value of axial force corresponds to compression force. It is noted that the maximum shear forces occur at the same time with the maximum compressional forces. The D-12 and D-12-V cases have almost the same axial force values. Consequently, it is reasonable to judge that the reduction for the D-12-V case is not attributed to the internal axial forces of piles. It may rather be associated with the external forces from neighboring soil behavior.

The soil behavior at this depth is investigated in **Fig. 11**, where only the maximum shear strain (γ_{xz}) and

normal stresses (σ_{xx} and σ_{zz}) are depicted. This figure indicates that the vertical excitation effect is negligibly small in the shear strain. However, the normal stresses decrease in the soil zone confined by piles. Therefore, the differences of the shear forces at G.L. –5 m can be attributed to soil normal stresses induced by the vertical excitation.

The axial force time histories of the L-12-V and L-12 are compared. The difference at the pier bottom under the sole horizontal excitation is small between them; however, it becomes large when the vertical excitation component is included simultaneously. The fluctuation for the L-12 case at pier bottom is below 2 per cent, while for the L-12-V case is 35 per cent. These values are calculated with respect to the static axial load. The effect of vertical excitation component in the piles is not visible in **Fig. 12.** Since the axial forces in piles are mainly induced by the footing rotation, they are practically the same values for both cases. In the analized bridge, the rotational constraint provided by the large number of piles renders the rocking component of foundation motion less significant. Moreover, at the pier, the L-12-V case has almost the same axial forces with the D-12-V case, which indicates the more significance of the axial force induced by the vertical excitation component than by the deck rotation. **Fig. 13** shows the distribution of the vertical acceleration along the transversal direction at the deck. Vertical responses of the outer piles include both an amplification of the pier's vertical movement and a geometric component of the rotational movement of the deck itself. The small variation of responses implies that the more predominant contribution to the vertical movements of deck comes from the rocking motion rather than from the vertical excitation.

(2) Deck eccentricity

From **Fig. 14**, it is noted that the cases with eccentricity attain the larger responses. If the shear force distribution of the D-12, D-12 (e=+1.5) and D-12 (e=-1.5) cases are compared, the maximum value at the pile top is attained in the D-12 (e=-1.5) case. The same tendency is noted for the bending moment but less recognizable. This indicates that the overturning moment produced by the superstructure is resisted more by the axial forces than by the bending of the piles, due to the rotational constraint condition provided by the gross of piles. When only the horizontal excitation component is considered in the analysis, the maximum bending moment appears at pier bottom for the D-12 case while at the pile top for the D-12 (e=-1.5) case. If the vertical excitation component is included simultaneously, the maximum values occur at the pier bottom for the D-12-V case and at the pile top for the D-12-V

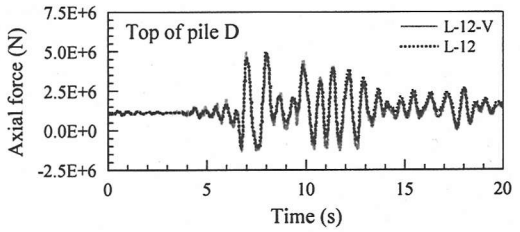

Fig. 12 Axial force time histories for the L-12 and L-12-V cases.

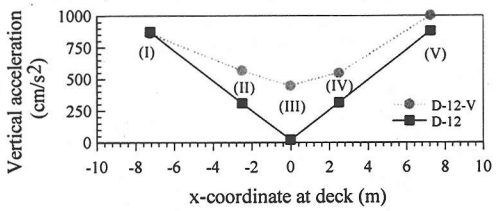

Fig. 13 Maximum vertical acceleration distribution along the deck.

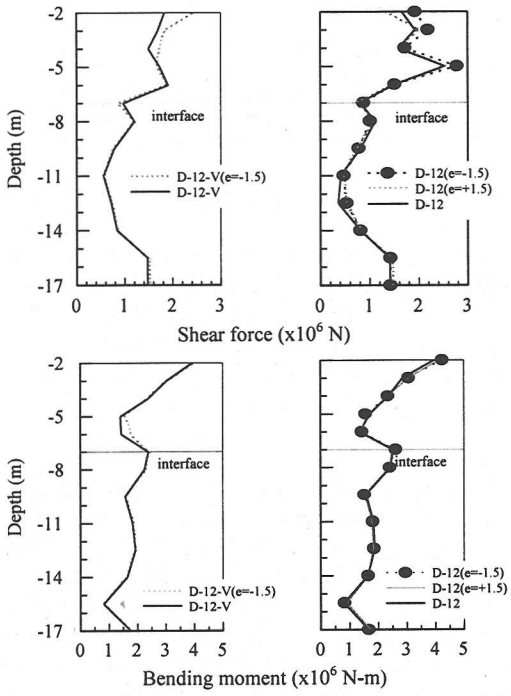

Fig. 14 Maximum horizontal displacement and internal force distribution to investigate the deck eccentricity effect.

(e=-1.5) case. Therefore, the cases without a deck eccentricity have the maximum responses at the pier bottom while the cases with a deck eccentricity attain the maximums at the pile top. From the view point of a possible structural damage, the deck eccentricity increases the ductility values at the pile top. They increase from 5.29 to 5.80 for the D-12 (e=-1.5) case. This implies that the damage by the deck eccentricity

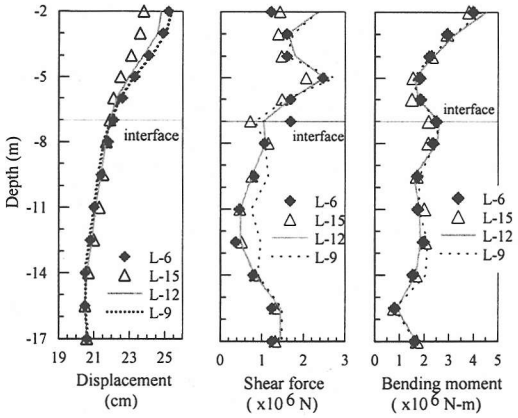

Fig. 15 Maximum horizontal displacement and internal force distribution to investigate the yield coefficient effect.

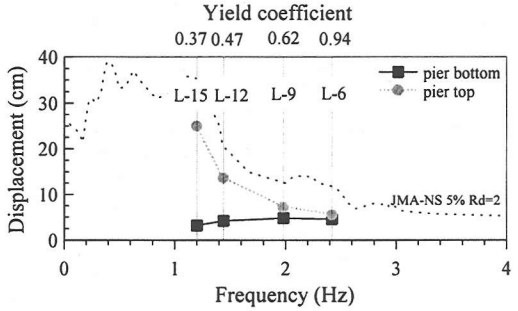

Fig. 16 Maximum horizontal displacement versus yield coefficient.

principally takes place at the foundation instead of at the pier.

(3) Structure flexibility

From **Fig. 15** for the internal force distribution the L-9 and L-12 cases have the largest shear forces at the pile top. It coincides with their largest inertial forces distribution. This is explained by the matching between the period range of the maximum pseudo acceleration spectral amplitudes and the fundamental periods of the L-9 and L-12 cases with fixed base condition. Obviously the maximum and minimum bending moments at the pier bottom correspond to the L-15 and L-6 cases, respectively. However, the same tendency is not noted at the pile top with the maximum values for the L-12 case and the minimum for the L-15 case. The overturning moment from the superstructure is principally resisted by the axial forces.

The maximum responses of the four cases versus the yield coefficient are shown in the following figures. Relative horizontal displacement envelopes with respect to the pile top are shown in **Fig. 16**. In this figure, the inelastic response spectrum for a reduction factor of 2 (5 % of damping) is also

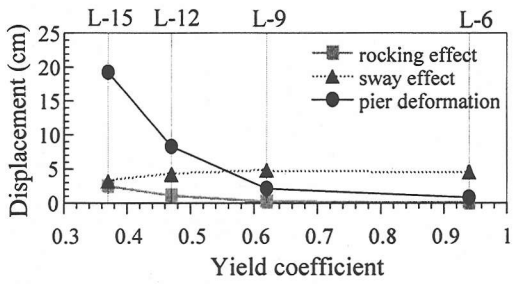

Fig. 17 Maximum relative pier top displacement components.

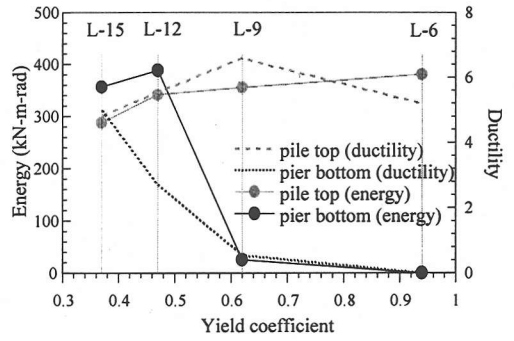

Fig. 18 Dissipated energy and ductility versus yield coefficient.

depicted. Since the pier response depends mainly on its flexibility for the rigid pier of the L-6, the displacement at pier top becomes smaller with almost the same value at the pier bottom. The horizontal displacements contain not only the pier deformation but also the displacements due to the sway and rocking of the foundation. Therefore, the total displacement is separated into these three components. **Fig. 17** shows the variation of these three types of displacement components. As the yield coefficient becomes higher, the pier deformation and rocking effects decrease, while the sway displacement increases gradually. It means that the sway effect is more important than the pier deformation when the pier is rigid. **Fig. 18** shows the maximum dissipated energy and the ductility values at the pile top and pier bottom. The dissipated energy at pile top are calculated from the sum of the 18 individual piles contribution. The rigidity (high yield coefficient) of the L-9 and L-6 cases results in almost null dissipation of energy at the pier. In contrast, the values at the pile top increase gradually with the yield coefficient. From the above considerations, the damage shifts from pier body to foundation in the case of high strength of the pier body.

6. EFFECTS OF SOIL PROFILE

Table 5 lists the cases investigated for the influence of the depth of interface of soft and stiff

Table 5 Soil profile cases.

CASE	Model	Soil profile
L-12	LUMP	Soil-12
L-21		Soil-21
L-11		Soil-11
L-22		Soil-22
L-12-s		Soil-12-s
L-12-d		Soil-12-d
L-21-s		Soil-21-s

CASE	Model	Soil profile
K-12	KINE	Soil-12
K-21		Soil-21
K-11		Soil-11
K-22		Soil-22
K-12-s		Soil-12-s
K-12-d		Soil-12-d
K-21-s		Soil-21-s

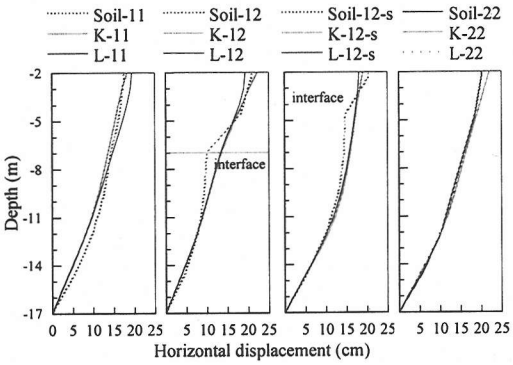

Fig. 19 Maximum horizontal displacement distribution along the pile (kinematic and total) and free soil for different soil profiles.

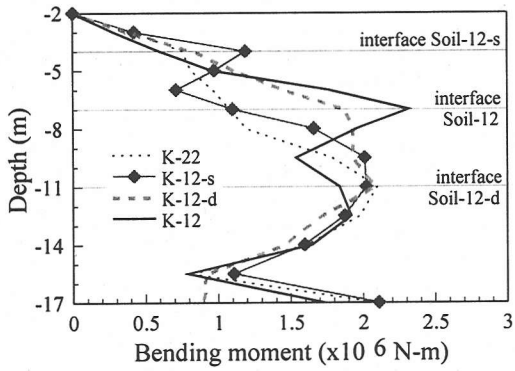

Fig. 20 Kinematic bending moment distribution along the pile length for soft soil on stiff soil.

layers (soft stratum on soft soil or vice versa) and frequency characteristics of the structural system.

Fig. 19 compares the horizontal displacements of the piles for the KINE and LUMP models, together with that of the free field in **Table 1**. The pile follows the free-field soil horizontal displacements in an average sense. Some deviations however exist, due to the irregularity of soil stiffness, near the ground surface and especially at the interface of layers for the Soil-12 and Soil-12-s profiles. When the interface of layers is located at –7 m (K-12), most of the amplification occurs at the upper soft layer. When the

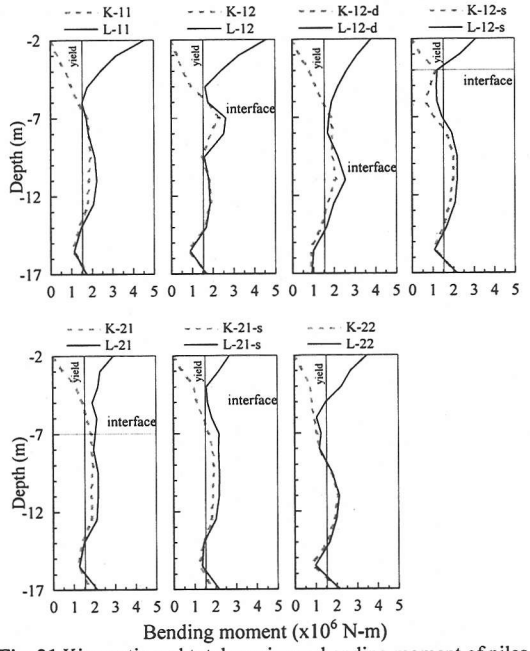

Fig. 21 Kinematic and total maximum bending moment of piles.

interface is at –4 m (K-12-s), the displacement profile attains a fairly uniform slope due to the thick soft stratum.

Fig. 20 plots the kinematic bending moment distributions along the pile length for homogeneous Soil-22 and soft layer underlain by stiff layer cases. When the soil is homogeneous (Soil-22), the bending moment profile is practically a parabolic distribution. If the layer interface is located close to the depth of maximum bending moment for the homogeneous soil, the bending moment distribution has also almost a parabolic distribution as noted for the K-12-d case. When the layers interface is located at –4 m or –7 m, the peak values appear at this depth (K-12 or K-12-s). **Fig. 21** shows the kinematic and total bending moment distributions along the pile length for all cases, where the vertical thin lines correspond to the yield bending moment under static axial load. Since the pile active length l_a for the inelastic behavior can be defined approximately by the depth at which the kinematic and total bending moments are equal, l_a is derived as 4~5 m for the structure-pile foundation in homogenous profile (Soil-11 and Soil-22). In a rigorously performed linear analysis, the kinematic and total bending moments at depths are almost identical since the load transmitted from the superstructure attenuate very rapidly with depth. However, when both surrounding soil and piles reach their yielding state, the kinematic and total bending moments are different even at depths, as noted for the structure with piles embedded in the Soil-21-s and Soil-12-d profiles. At the interface of the Soil-21-s

profile, the differences between L-21-s and K-21-s responses are due to the superstructural inertia force since its pile active length is larger than thickness of first soil layer.

The previously mentioned bending moment peaks at interface for the K-12 and K-12-s cases (soft layer on stiff layer) do not appear for the K-21 and K-21-s cases (stiff layer on soft layer) as is shown in **Fig. 22**. This figure compares the bending moment distribution for homogeneous Soil-11 and stiff layer underlain by soft layer cases Soil-21 and Soil-21-s. The bending moment distribution for these cases and the K-11 case are almost the same. The stiff layer underlain by soft layer leads to the smaller amplification than the soft layer on stiff layer. The supporting interpretation is made from the maximum shear strain of the soil in **Fig. 23**. In this figure, x=-0.63 m corresponds to the soil between the internal piles, x=-4.25 m to the soil near the outer side of external pile and x=-9.5 m to the soil far away from the foundation. It is noted that the Soil-12 profile generates a larger response than the Soil-21 profile, especially at interface between layers. Therefore, a soft surface layer underlain by a stiff soil stratum is crucial to the above behavior.

The relationship between the location of the soft and stiff layers and the possible degree of damage is investigated by taking account of the ductility values for pile and pier. The results in **Fig. 24** are shown in two groups: one ground composed of soft soil underlain by stiff layer (L-21 and L-21-s) and the other ground composed in the opposite way (L-12-d, L-12 and L-12-s). While large plasticity values are noted for the piles embedded in soft soils (L-11 or L-12-d), these values are reduced when a stiff layer is deposited on a soft soil (L-21 or L-21-s) or when the soil becomes stiffer (L-12-s or L-22). In contrast to the big variation of the values at pile, the variation at pier bottom is small.

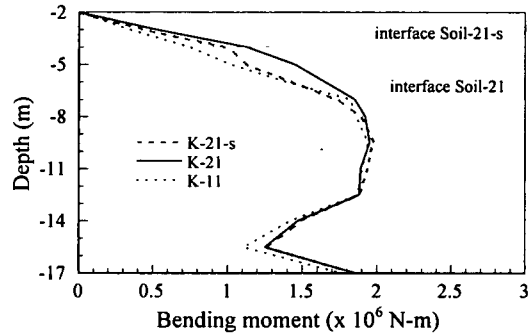

Fig. 22 Kinematic bending moment distribution along the pile length for stiff soil on soft soil.

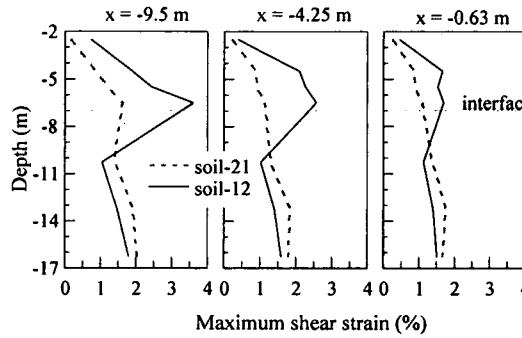

Fig. 23 Maximum shear strain of soil.

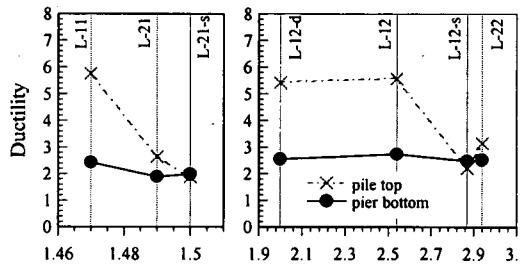

Fig. 24 Ductility versus natural soil frequency at the pile top and pier bottom for different soil profiles.

7. CONCLUSIONS

Effect of the superstructure characteristics on piles is significant when they are in inelastic behavior. The reverse effect is so small that the damage degree at the pier is not affected by the pile behavior; rather it is governed dominantly by the girder inertia. The inelastic behavior of piles results in different internal forces among the piles mainly due to the axial force, while for the elastic behavior the internal piles were the same and the external piles Special attention should be paid to the cases where an increase of the inelastic behavior of the piles is more probable when the second mode of the interaction system is strong and when structures have a deck eccentricity.

The predominant contribution to the vertical response at the deck comes from the deck rocking rather than from the vertical excitation. The axial force at pier is mainly induced by the vertical excitation input than by the deck rotation. The vertical excitation reduces the shear forces at piles, which is associated with the reduction of normal stresses in the soil confined by piles. The possible failure of piles is due to the relation between compression force with bending moment rather than tension force with bending moment.

The negative effects of an unbalanced design (very rigid superstructure and flexible piles or vice versa) between the superstructure and the piles have been demonstrated. Large shear forces at the pile top might be crucial to lead a possible shear-bending

failure type. High yield coefficient value at pier that defines the quotient of the horizontal yield load to the weight of superstructure increases the inelastic behavior of piles, so that the portion susceptible to damage shifts from the pier to the piles. The energy dissipated by piles increase gradually with the yield coefficient. Parametric chart for dissipated energy or for ductility versus yield coefficient at pile and pier, can be of use in getting the balancing.

The inelastic kinematic interaction between soil and pile has been shown. The magnitude of the bending moment developed in piles is substantial at the interface of a shallow soft layer with an underlying stiff layer. Therefore, piles should be designed against more unfavorable condition.

The conclusions drawn from the parametric studies can not be generalized to bridges and soil deposits with characteristics vastly different from these of the studied cases. However, the results of this study might help qualitatively in the understanding and prediction of the complicated SPSI behavior, which can contribute to improve the design practice.

REFERENCES

1) Mizuno, H., Iiba, M. and Hirade, T.: Pile damage during the 1995 Hyogo-ken Nanbu Earthquake in Japan, *Proceedings of the 11th World Conference on Earthquake Engineering*, Acapulco, Mexico, Paper No. 977, 1996.

2) Tokimatsu, K., Mizuno, H. and Kakurai, M.: Building damage associated with Geotechnical problems, *Soils and Foundations, Special Issue on Geotechnical Aspects of the January 17, 1995 Hyogo-ken Nanbu Earthquake, JSCE*, pp. 219-234, 1996.

3) Maki, T., Takano, K. and Mutsuyoshi, H.: Response analysis of reinforced concrete pier with pile footing considering nonlinear soil, *Proceedings of the 7th East Asia-Pacific Conference on Structural Engineering & Construction*, Japan, pp. 746-751, 1999.

4) Murono, Y. and Nishimura, A.: Evaluation of seismic force of pile foundation induced by inertial and kinematic interaction, *Proceedings of the 12th World Conference on Earthquake Engineering*, Auckland, New Zealand, Paper No. 1496, 2000.

5) Kavvadas, M. and Gazetas, G.: Kinematic seismic response and bending of free head piles in layered soil, *Géotechnique*, Vol. 43, No. 2, pp. 207-222, 1993.

6) Mylonakis, G., Nikolaou, A. and Gazetas, G.: Soil-pile-bridge seismic interaction: kinematic and inertial effects. Part I: soft soil, *Earthquake Engineering and structural Dynamics*, Vol. 26, pp. 337-359, 1997.

7) Takemiya, H. and Adam, M.: 2D nonlinear seismic ground analysis by FEM-BEM: The case of Kobe in Hyogo-ken Nanbu earthquake, *Proceedings of the JSCE*, No.584/I-42, pp. 19-27, 1998.

8) Hardin, B.O. and Drnevich, V.P. : Shear modulus and damping in soils: design equations and curves, *Journal of the Soil Mechanics and Foundations Division*, ASCE, Vol. 98, SM7, pp. 667-692, 1972.

9) Takemiya, H., Maotian, L. and Gao, L.: 2-D nonlinear seismic response of soil structures with emphasis on local topography, *Report submitted to Monbusho International Scientific Research Program*, Grant No. 0104409, 1991.

10) Giberson, M.F.: Two nonlinear beams with definitions of ductility, *Journal of the Structural Division, Proceedings of the American Society of Civil Engineers*, Vol. 95, ST2, pp. 137-157, 1969.

11) Takemiya, H. and Shimabuku, J.: Nonlinear seismic damage analysis of bridge pier supported by piles, *The 10th Earthquake Engineering Symposium Proceedings*, Vol. 2, Yokohama, Japan, pp. 1687-1692, 1998.

12) Saidi, M. and Sozen, M. A.: Simple and complex models for nonlinear seismic response of reinforced concrete structures, *Structural Research Series No. 465*, Civil Engineering Studies, University of Illinois, Urbana, 1979.

13) Shimabuku, J. and Takemiya, H.: Nonlinear soil-pile foundation interaction analysis based on FEM-BEM hybrid technique, *Proceedings of the 25th JSCE Earthquake Engineering Symposium*, Tokyo, Japan, pp. 461-464, 1999.

14) Japan Road Association: *Design Specifications of Highway Bridges, Part IV. Substructure Design*, 1996.

15) Japan Road Association: *Design Specifications of Highway Bridges, Part V. Seismic Design*, 1996.

(Received February 26, 2001)

上部構造と成層地盤の影響における杭基礎-橋脚系の非線形地震応答性状

Jorge SHIMABUKU・竹宮宏和

本研究は，上部構造と杭と地盤の非線形動的相互作用を扱ったものである．地震時，上部構造－杭基礎－地盤系の連成解析から，各部分の特性が他の応答へ及ぼす効果に注目して応答性状を調べた．その結果，杭が非線形挙動を示す場合，杭が上部構造のいろいろな特性の影響を受け，特に，杭が非線形挙動を示す可能性の高い強い2次固有モードとなる構造物と，デッキが偏心を持っている構造物でその傾向が強いこと，逆に杭から橋脚への影響は少ないことが分かった．橋脚の降伏係数（自重に対する降伏力）が高い場合，杭が非線形挙動を示す可能性が大きくなる．地盤変形による杭体曲げモーメントは，固い地盤の上に浅く柔らかい地盤がある時の地盤物性値が急変する所でピークになる．